Molecular Therapy
Original Article

Contribution of Implanted, Genetically Modified Muscle Progenitor Cells Expressing BMP-2 to New Bone Formation in a Rat Osseous Defect

Rodolfo E. De La Vega,[1,2] Consuelo Lopez De Padilla,[1] Miguel Trujillo,[1] Nicholas Quirk,[1] Ryan M. Porter,[2] Christopher H. Evans,[1,2,3] and Elisabeth Ferreira[2]

[1]Rehabilitation Medicine Research Center, Mayo Clinic, Rochester, MN 55905, USA; [2]Center for Advanced Orthopaedic Studies, BIDMC, Boston, MA 02215, USA; [3]Collaborative Research Center, AO Foundation, Davos, Switzerland

Because muscle contains osteoprogenitor cells and has a propensity to form bone, we have explored its utility in healing large osseous defects. Healing is achieved by the insertion of muscle fragments transduced with adenovirus encoding BMP-2 (Ad.BMP-2). However, it is not known whether the genetically modified muscle contributes osteoprogenitor cells to healing defects or merely serves as a local source of BMP-2. This question is part of the larger debate on the fate of progenitor cells introduced into sites of tissue damage to promote regeneration. To address this issue, we harvested fragments of muscle from rats constitutively expressing GFP, transduced them with Ad.BMP-2, and implanted them into femoral defects in wild-type rats under various conditions. GFP$^+$ cells persisted within defects for the entire 8 weeks of the experiments. In the absence of bone formation, these cells presented as fibroblasts. When bone was formed, GFP$^+$ cells were present as osteoblasts and osteocytes and also among the lining cells of new blood vessels. The genetically modified muscle thus contributed progenitor cells as well as BMP-2 to the healing defect, a property of great significance in light of the extensive damage to soft tissue and consequent loss of endogenous progenitors in problematic fractures.

INTRODUCTION

Large segmental defects in bone do not heal well and remain a pressing clinical problem.[1] Much research addresses this matter through approaches based on mechanobiology, tissue engineering, regenerative medicine, and gene therapy.[2–6]

Attention has been drawn to the remarkable osteogenic properties of skeletal muscle, as manifest in the genetic disease fibrodysplasia ossificans progressiva (FOP),[7] and the high incidence of heterotopic ossification after blast injuries and surgical replacement of the hip and elbow.[8] FOP results from an activating mutation in the activin receptor A type I, a bone morphogenetic protein (BMP) type I receptor.[9] This suggests that human muscle forms bone very effectively in the presence of a sustained BMP signal. Based on this information, we have explored the possibility to heal critical-sized defects in rat femora by the implantation of muscle discs transduced with a recombinant adenovirus carrying BMP-2 cDNA (Ad.BMP-2). Results so far have been promising in this model.[10,11]

Healing of defects in this fashion occurs via endochondral ossification,[11] but little else is known about the biology of healing. A pressing question, of general importance to the field of regenerative medicine, is whether the implanted cells heal indirectly by acting as transient local sources of paracrine factors or whether progenitor cells within the implant remain at the defect site and form new tissue directly. Although the field of tissue engineering was predicated on the latter assumption, recent evidence suggests that regeneration is largely a result of host cells acting under the paracrine influence of introduced cells that quickly disappear. The present study was designed primarily to address this question.

This matter is not merely academic. Problematic fractures, including segmental defects, are often associated with substantial injury to surrounding soft tissue, which reduces the population of local progenitor cells available for bone healing. Under these circumstances, an implant providing both persisting osteogenic cells and sustained osteogenic signals would be highly advantageous.

At the time this study was initiated, the only genetically modified rats available for this type of research expressed GFP in all cells.[12] These were thus used to explore the fate of donor muscle cells after implantation into critical-sized defects in host femora.

RESULTS

Transduction of Muscle Discs

The study design is outlined in Figure 1. Skeletal muscle was harvested from rats and punched into discs 4 mm in diameter and

Received 26 May 2017; accepted 1 October 2017;
https://doi.org/10.1016/j.ymthe.2017.10.001.

Correspondence: Christopher H. Evans, Rehabilitation Medicine Research Center, Mayo Clinic, 200 First Street SW, Rochester, MN 55905, USA.
E-mail: evans.christopher@mayo.edu

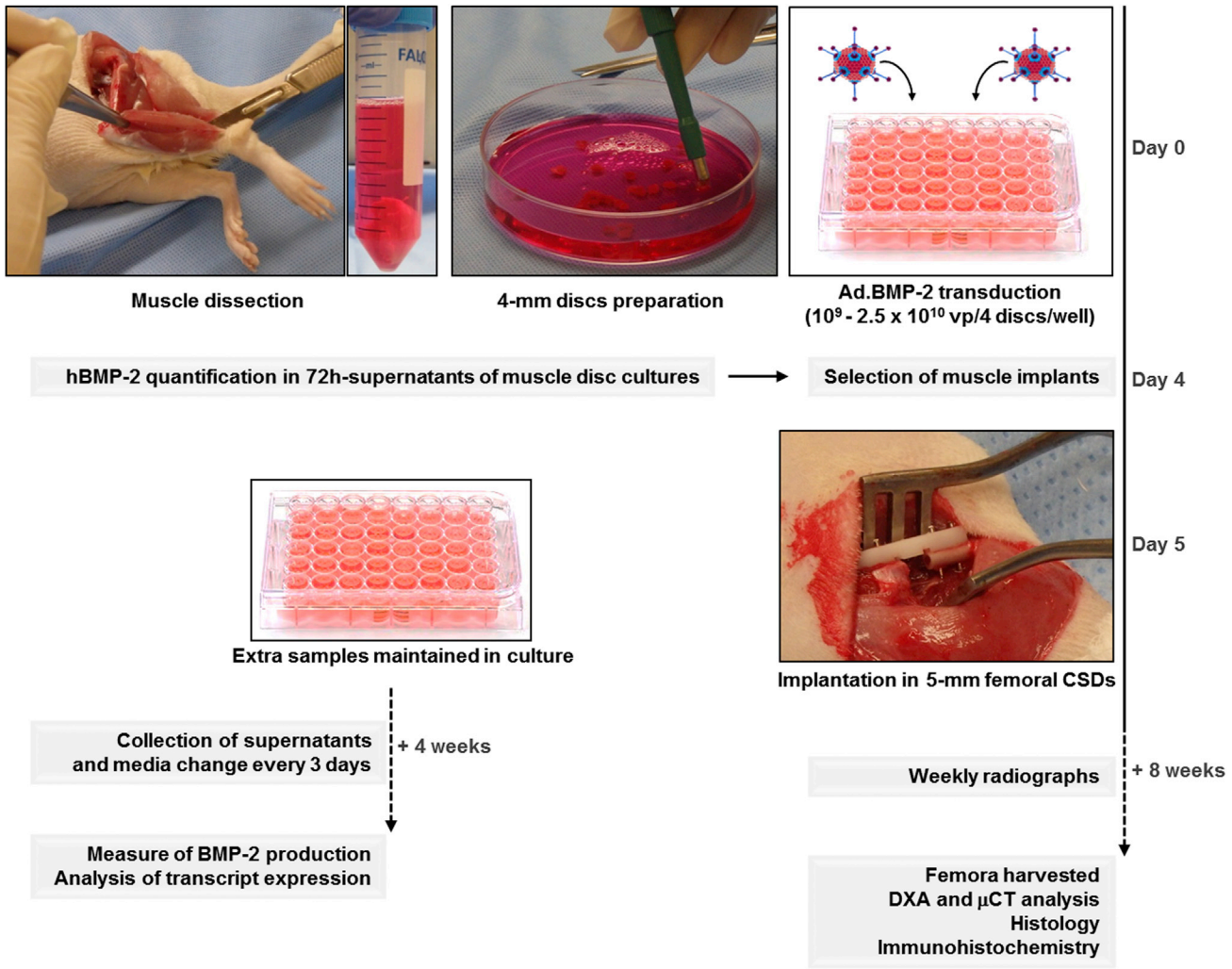

Figure 1. Experimental Design

Muscle discs were recovered from GFP$^+$ rats, transduced with Ad.BMP-2, and inserted into surgically created critical-sized defects (CSDs) in the femora of wild-type rats. Other discs from the same batch were maintained in culture, and BMP-2 secretion was measured for up to 4 weeks. Healing of defects in rats was monitored by weekly X-ray. After 8 weeks, femora were harvested and examined for bone bridging and the presence of GFP$^+$ donor cells within wild-type recipient defects.

2–3 mm thick. These were transduced with Ad.BMP-2 at doses ranging from 10^9 to 2.5×10^{10} viral particles (vp)/4 discs leading to the secretion of 8.04 ± 0.86 to 138.19 ± 2.0 ng BMP-2/48 hr/4 discs at day 3 after transduction. At the time of implantation (i.e., day 5), discs produced from 87 ± 6.28 to 336.11 ± 188.41 ng BMP-2/48 hr/implant. Production of BMP-2 persisted for at least 28 days in vitro (Figure S1A).

RT-PCR revealed strong, increased expression of transcripts encoding alkaline phosphatase and osteocalcin, with more modest increases in runx2 and osteopontin (Figure 2A) in disc cultures 4 weeks after transduction. Col1A1 levels were not significantly altered by BMP-2 overexpression. Transcripts encoding human BMP-2 were also highly elevated, while the rat isoform was downregulated (Figure 2B).

Bone Healing Using Genetically Modified Muscle

Healing was monitored by weekly X-ray and assessed as complete bridging when there was osseous callus filling the entire defect, partial bridging when callus was present but failed to fill the defect, or no bridging when there was no evident callus response after 8 weeks (Figure 3A). Complete bridging was observed uniformly in rats receiving 11 µg recombinant human (rh) BMP-2, which is a well-established positive control for this model.

In a first series of experiments, Ad.BMP-2-transduced muscle discs derived from GFP$^+$ rats were implanted into femoral defects in wild-type recipients. Of 28 defects treated in this fashion, only 2 achieved radiologic bridging. Eight animals mounted a partial bridging response and the rest did not form new bone (data not shown).

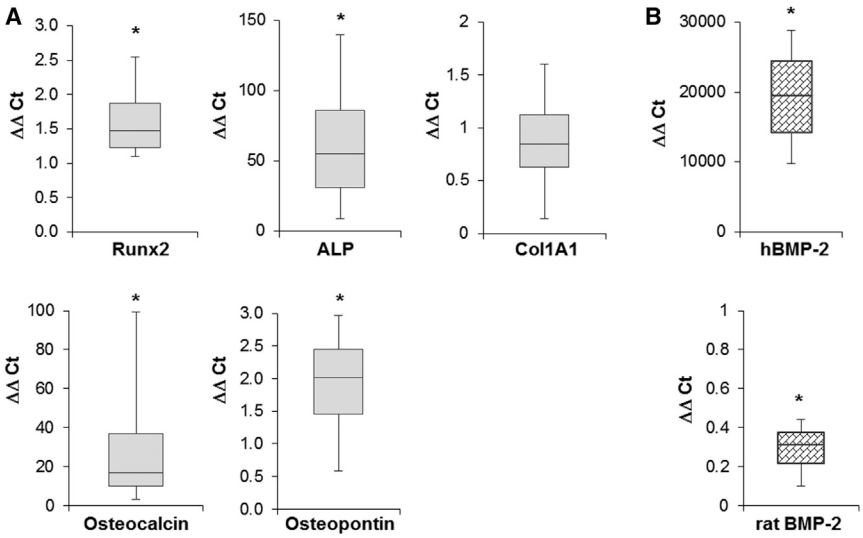

Figure 2. In Vitro Expression of Bone-Related Transcripts and BMP-2 by Muscle Disc Cultures

(A) mRNA expression of bone-related genes. RT-PCR was used to measure the relative expression of the bone-related marker genes ALP, Runx2, col1A1, osteocalcin, and osteopontin in muscle discs transduced with Ad.BMP-2 (n = 8). (B) mRNA expression of human and rat BMP-2 transcripts (n = 8). mRNA expression levels were normalized to those of the internal standard GAPDH, and they are reported as relative values (ΔΔCT) to those obtained from the cultures of untransduced muscle discs. Asterisks indicate statistically significant difference ($p < 0.05$) from controls. Representative results are shown as box and whisker plots, with median as the horizontal bar, interquartile range calculated using Tukey hinges as the box, and the lowest and highest values represented as whiskers.

GFP is a foreign protein to wild-type animals. Because our previous work suggests that bone healing in this model is highly sensitive to activation of the immune system,[10,11] additional experiments were conducted to determine whether immune responses influenced healing. In one experiment to address this possibility, transduced muscle from GFP^+ rats was transplanted into wild-type recipients that were immunosuppressed with a combination of FK506 and SEW2871.[10] All 7 wild-type animals receiving transduced, GFP^+ muscle with immunosuppression bridged their defects (Table S1).

To examine further the possible influence of the immune system, muscle discs from GFP^+ rats were transduced with Ad.BMP-2 and implanted into GFP^+ recipients in the absence of immunosuppression (Table S1). Partial bridging occurred in 3 of 4 GFP^+ rats receiving transduced GFP^+ muscle grafts. The fourth animal was euthanized because of implant pin loosening.

Comparison of the amount of BMP-2 produced by discs in relation to whether or not they bridged revealed that, below a threshold of about 15 ng BMP-2/48 hr/4 discs, no bone was formed (Figure S1B). Once BMP-2 expression exceeded approximately 25 ng BMP-2/48 hr/4 discs, new bone was formed, although this did not always lead to radiologic bridging of defects (Figure S1B). This suggests that factors other than BMP-2 production help determine whether bridging occurs or not.

Histology

Histological examination confirmed that defects that failed to bridge were filled with fibrous connective tissue (Figures 3B–3D). Under conditions of partial bridging, areas of new bone were interspersed with fibrous tissue. Occasional areas of cartilage were noted. Bridged defects showed restoration of cortices with the formation of marrow elements (Figure 3B). None of the samples showed evidence of a severe inflammatory response.

Microcomputed Tomography and Dual-Energy X-Ray Absorptiometry

Microcomputed tomography (μCT) images (Figure 4) confirmed the restoration of osseous continuity, with cortication, both in defects bridged with rhBMP-2 and defects bridged with genetically modified muscle. Axial images of defects completely bridged using genetically modified muscle were closer in appearance to those of native bone than images of defects bridged with rhBMP-2. In the latter cases, new bone formation expanded outside the defect area, surrounding the fixation plate.

Quantitative analysis of the μCT data confirmed that the bone volume and total volume were closer to normal for defects bridged with muscle grafts than those bridged with rhBMP-2 (Figure 5A). The polar moment of inertia was also closer to normal values (Figure 5B).

Dual-energy X-ray absorptiometry (DXA) analysis showed that bone formed with genetically modified muscle had lower bone mineral content than intact femora (Figure 5C).

Fate of Implanted Muscle Cells

Immunohistochemistry was used to identify GFP^+ cells within wild-type recipient rats. Isotype control antibody showed no cross-reactivity. The range of healing responses noted above (Figure 3) allowed the examination of defects with various degrees of bridging (Figures 6, 7, and 8).

In defects that failed to form new bone, GFP^+ cells were identified as fibroblastic cells within a non-mineralized connective tissue matrix (Figure 6). In partially bridged defects (Figure 7) and fully bridged defects (Figure 8), the newly formed bone contained a mixture of donor and host cells. Some partially bridged defects also contained areas of cartilage (Figure 7), the chondrocytes being of both host and donor origin. Chondrogenesis of endogenous progenitors may have been

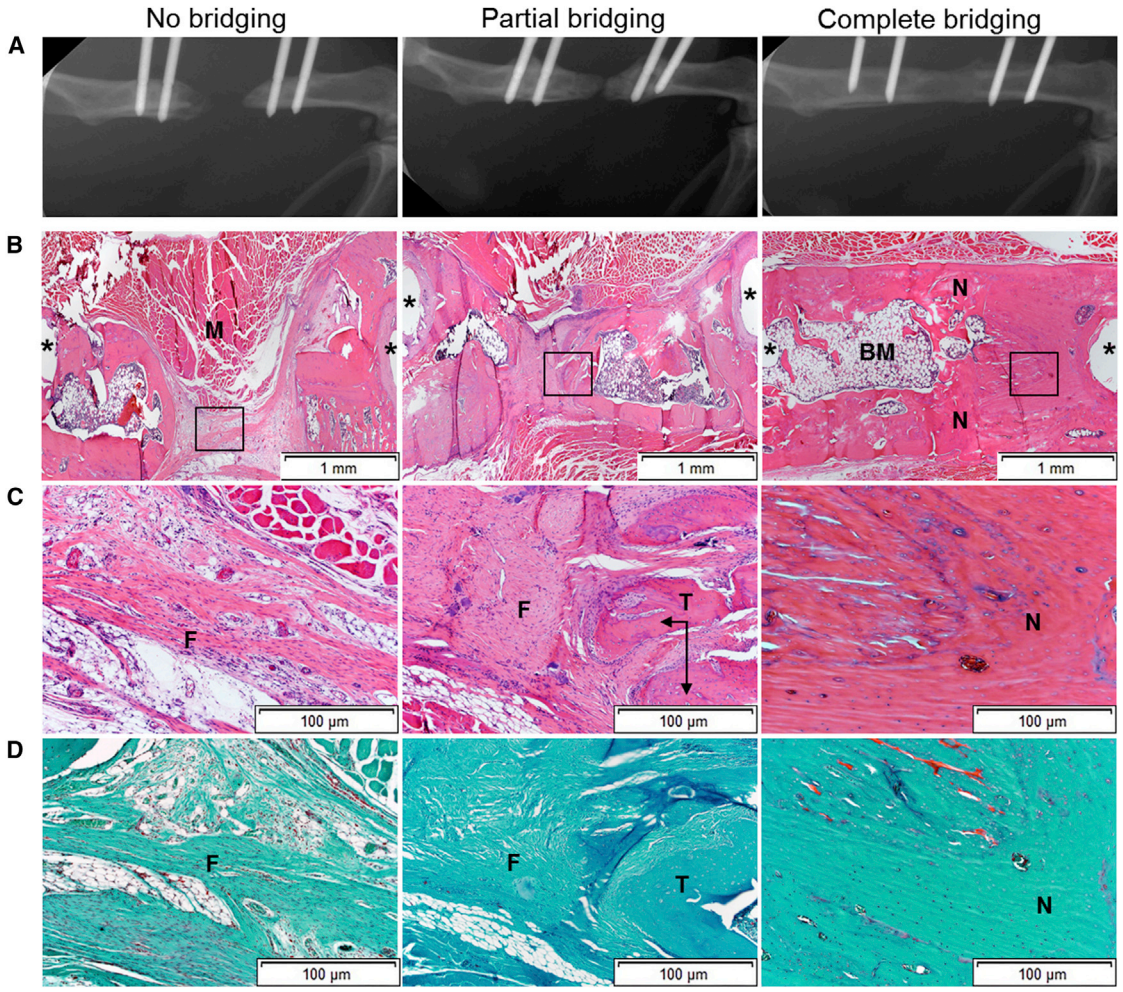

Figure 3. Radiologic and Histologic Analyses of Bone Healing

(A) After 8 weeks, femora underwent their final X-rays and rats were euthanized. (B–D) Defects that failed to bridge, underwent partial bridging, or progressed to complete bridging were sectioned and stained with H&E (B and C) or SOFG (D). The boxed areas of the images in (B) are shown at higher magnification in (C) and (D). N, new bone; M, muscle; F, fibrous tissue; T, trabecular bone; BM, bone marrow. Asterisks show site of pinholes.

favored by the unstable mechanical conditions of these non-unions. Areas of apparent endochondral ossification were also visible. GFP^+ cells were also noted lining the internal surfaces of newly formed blood vessels (Figure 7).

Host and donor cells from six different areas within the newly formed bone from two samples per group were counted; 64.1% ± 21.9% of cells within the new bone of partially bridged defects were of donor origin, whereas 76.2% ± 8% of cells within the new bone of completely bridged defects were of donor origin.

DISCUSSION

The primary goal of this investigation was to determine whether new bone formed within critical-sized defects after the implantation of genetically modified muscle discs expressing BMP-2 is of host or donor cell origin. This issue is pertinent to the wider discussion of whether exogenously supplied progenitor cells contribute to tissue regeneration by forming new tissue via differentiation and incorporation or whether they serve as a transient source of paracrine factors and then disappear. The latter interpretation is increasingly favored. Our data, however, confirm that the donor cells present in fragments of skeletal muscle persist in the host defect site, and they do so regardless of whether or not they form bone.

Donor cells may have survived in the host because their micro-niches within muscle were not destroyed during preparation of the genetically modified tissue for implantation.[13] Many regenerative medicine protocols, in contrast, enzymatically digest donor tissue to liberate progenitor cells, a process that destroys these niches. The behavior of the isolated cells may be further altered by serial expansion in vitro. For use in tissue regeneration, such cells are frequently delivered as suspensions or seeded onto manufactured scaffolds. Under

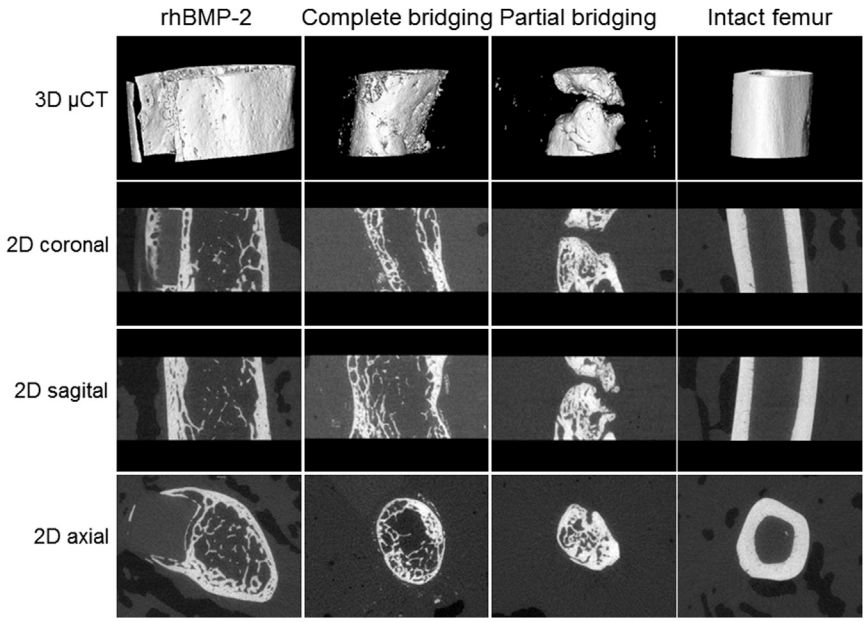

Figure 4. Imaging of Defects by Microcomputed Tomography

After 8 weeks, animals were euthanized, and the operated and contra-lateral femora were recovered and imaged as described in the Materials and Methods.

these circumstances, the transplanted cells may lack the survival signals of their native environments.[13]

In the absence of a sufficient osteogenic stimulus, the implanted cells persisted as fibroblasts within a fibrous connective tissue. When bone was formed, the donor cells appeared to contribute to several different cell types, including osteocytes, osteoblasts, chondrocytes, and endothelial cells lining new blood vessels. As noted in the Introduction, the ability of the implanted tissue to provide progenitor cells that differentiate into cells of the repair tissue is a considerable advantage when healing defects where local progenitors have been damaged through injury or, in the case of tumor resection, irradiation.

The representation of donor cells in newly formed bone varied between approximately 60% and 75%. Because samples were examined by immunohistochemistry after 8 weeks, we do not know whether the initial representation of donor cells was higher, with progressive replacement by host cells as the newly formed woven bone was remodeled. It has been known for a long time that skeletal muscle contains osteoprogenitor cells,[14] but the identity of the progenitor cells within skeletal muscle that formed new tissue in the present experiment was not investigated here; candidates include satellite cells,[15] mesenchymal stem cells,[16] muscle-derived stem cells,[17] and endothelial lining cells from blood vessels within muscle.[18]

Our data are also relevant to a discussion of the fate of chondrocytes during endochondral ossification, the mechanism through which the appendicular skeleton develops,[19] fractures heal,[20] heteropic ossification develops in FOP,[7] and genetically modified muscle forms bone in rat femora.[11] The received view, that hypertrophic chondrocytes undergo apoptosis and are replaced by osteoblast progenitors from the circulation,[21] has been challenged.[22–24] Recent data suggest that there are circumstances where hypertrophic chondrocytes survive and differentiate into osteoblasts, some of which, in due course, become osteocytes.[23,24] Our data strongly support this postulate.

Although not the primary focus of this study, our data again draw attention to the sensitivity of bone healing to immune activation. Historically, we have noted this when injecting Ad.BMP-2 directly into mice,[25] rats,[26] and sheep[27,28] and also when developing the genetically modified muscle technology described here. For instance, muscle transfers of this kind were only partially successful in Sprague-Dawley rats, which are not syngeneic, but fully successfully in Fischer rats, which are.[11] In a previous study, we immunosuppressed recipient rats with FK506 and SEW2871 to allow xenografting of sheep muscle.[10] Under these conditions, bone healing was enhanced beyond that expected from improved xenografting alone. Likewise, in the present study, bone bridging following the implantation of GFP^+ muscle into wild-type rats in the presence of FK506 and SEW2871 was superior to that occurring when GFP^+ muscle was transplanted into GFP^+ hosts in their absence.

We originally suspected that GFP^+ donor cells were being rejected by wild-type recipient rats to whom GFP is a foreign antigen. But immunohistochemistry showed that GFP^+ cells endured in non-immunosuppressed, wild-type animals. The cells persisted as fibroblasts, suggesting a role for immunosuppression in promoting osteogenesis rather than enabling tissue grafting. However, further analysis is complicated by the leaky nature of the first-generation adenovirus vectors used in this study. Despite deletions in the E1 and E3 regions of the genome, a low level of viral proteins is still produced by transduced cells, generating a cell-mediated immune response.[29] Because only a fraction of the muscle disc cells is transduced by adenovirus, there is a population of non-transduced GFP^+ cells that could remain in the defect under conditions of immunoreactivity to adenoviral antigens. The deleterious effects of immune activation are also suggested by the work of Reinke et al.,[30] who reported that bone healing is inhibited by $CD8^+$ memory T cells. Osteogenic responses to BMP-2 may also benefit from the interaction of FK506 with its binding protein 12 (FKBP12), which amplifies intra-cellular signal transduction via the BMP receptor.[31,32] These additional factors help explain why healing was not only predicated on the amount of BMP-2 that was produced by the implanted muscle discs.

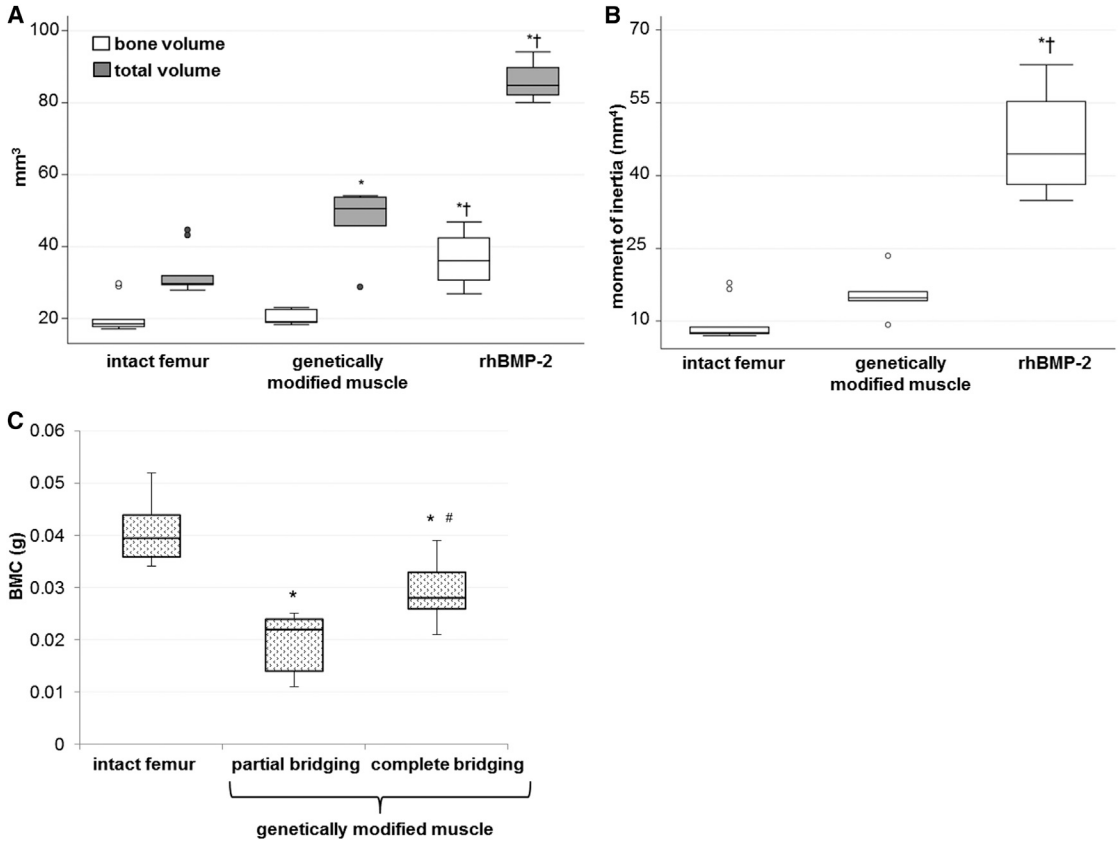

Figure 5. Quantitative μCT and DXA Data

(A) Bone volume and total volume of intact femora and defect sites healed with BMP-2 or genetically modified muscle discs were determined from μCT data (n = 11 animals). (B) Polar moment of inertia of intact femora and defect sites bridged with BMP-2 or genetically modified muscle discs calculated from μCT data (n = 11 animals). *p < 0.05 compared to the intact femur group; †p < 0.05 compared to the genetically modified muscle group. (C) Bone mineral content (g) of intact femora and defect sites bridged or partially bridged using genetically modified muscle discs (n = 11). *p < 0.05 compared to the intact femur group; #p < 0.05 compared to the partial bridging group. Representative results are shown as box and whisker plots, with median as the horizontal bar, interquartile range calculated using Tukey hinges as the box, and the lowest and highest values represented as whiskers.

The technology described here holds promise as a means of repairing osseous defects in which the pool of endogenous osteoprogenitor cells is depleted. Suitably adapted, the method could permit point-of-care delivery in which autologous muscle would be harvested, genetically modified, and implanted intra-operatively into osseous defects. An expedited approach such as this would greatly facilitate clinical application.[33] In previous work, we have noted that genetically modified fat has a certain ability to heal experimental osseous lesions in the manner described here for muscle.[10,11] Use of adipose tissue would further facilitate clinical translation. Regardless of the donor tissue of choice, the protocol will need optimizing and evaluating in a large animal model before progressing to human trials.

MATERIALS AND METHODS

Animals

F344-Tg(UBC-EGFP)F455Rrrc rats (*Rattus norvegicus*, RRC strain 307) were acquired from the Rat Resource and Research Center (RRRC, University of Missouri, MO) and bred at the institutional animal care facility. Male (wild-type) Fischer F344 rats were purchased from Charles River Laboratory (Wilmington, MA). All animals were housed in a central animal care facility with 12-hr light cycles and were given chow and water ad libitum. Animal care and experimental protocols were followed in accordance with NIH guidelines and approved by the Beth Israel Deaconess Medical Center Institutional Animal Care and Use Committee.

Preparation of Genetically Modified EGFP Muscle Discs

Skeletal muscle was harvested aseptically from biceps, *vastus lateralis*, *soleus*, and *gastrocnemius* muscles of 20-week-old EGFP rats and punched into discs of 4-mm diameter and 2- to 3-mm depth. These were transduced with a first-generation adenovirus (ΔE1, ΔE3), serotype 5, carrying the human BMP-2 cDNA (Ad.BMP-2)[34] at doses ranging from 10^9 to 2.5×10^{10} vp/4 discs. Briefly, discs were transferred to wells of a 48-well plate, and 100 μL virus suspension was added in low-glucose (1 g/dL) DMEM (LG-DMEM, Mediatech, Manassas, VA) supplemented with 0.1% fetal bovine serum (FBS;

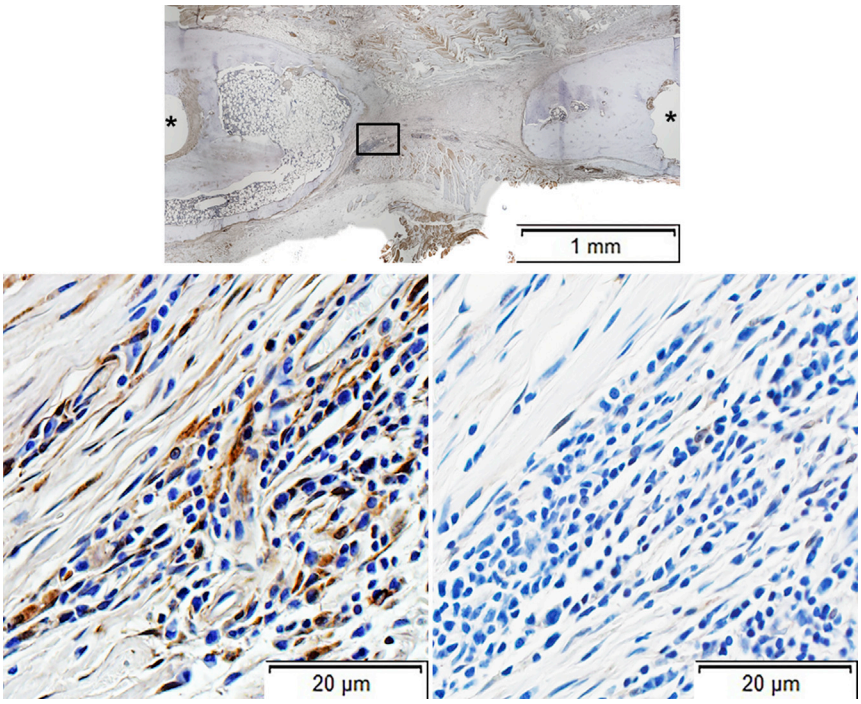

Figure 6. Immunohistochemical Analysis of Defects Where No Bridging Occurred

Sections were stained with anti-GFP antibody (top and left bottom panels). As confirmed in the top panel, this defect did not bridge. Examination under higher power (left bottom panel) revealed GFP^+ fibroblastic cells within a fibrous connective tissue. Isotype control antibody failed to stain any cells (right bottom panel). Asterisks show sites of pinholes.

HyClone, Logan, UT) and centrifuged at 2,000 × *g* for 30 min (37°C). Discs were then incubated at 37°C/5% CO_2 for 210 min before the removal of virus-containing media and the addition of complete media, consisting of LG-DMEM supplemented with 10% FBS and 50 μg/mL ascorbic acid-2-phosphate (Sigma-Aldrich, St. Louis, MO). BMP-2 production was quantified in 72-hr muscle supernatants using the human BMP-2 DuoSet ELISA kit (R&D Systems, Minneapolis, MN). Discs were either implanted into critical-sized defects 96 hr after transduction or maintained in culture for 4 weeks. Cultures were supplemented with 10 mM glycerophosphate (Sigma-Aldrich) after 10 days of osteogenic culture. Supernatants were collected regularly for quantification of BMP-2 secretion.

Surgical Procedure

Wild-type rats were 15 weeks of age at the time of surgery. A 5-mm, critical-sized, mid-femoral defect was created in the right hind limb of each rat. Under sterile conditions, a 4-cm incision was made on the posterolateral thigh. The lateral intermuscular septum with respect to the femur was dissected to expose the diaphysis of the femur. Care was taken to preserve the periosteum and the surrounding soft tissues. Using a polyacetal plate[35] (Special Designs, La Vernia, TX) as a guide, four holes were drilled along the mid-diaphysis using a 0.79-mm drill bit. The plate was then secured carefully to the femur using four hand-driven 0.9-mm threaded K-wires (MicroAire Surgical Instruments, Charlottesville, Virginia), which allowed the construct to act as a locked plate. A 5-mm osteotomy was placed precisely equidistant from each of the inner wires using a 0.22-mm Gigli wire saw (RISystem AG, Davos Platz, Switzerland) and a precision saw guide. After completion of the osteotomy, the site was irrigated with saline, and 4 discs of genetically modified EGFP muscle were press-fit in the 5-mm gap. Positive controls received 11 μg rhBMP-2 (Medtronic, Dublin, Ireland) soaked in a collagen type I sponge (Integra LifeSciences, Plainsboro, NJ). A soft tissue pouch was created using the adjacent muscles to ensure the muscle graft and collagen sponge would stay in place. The wound was closed in layers with 4-0 Vicryl sutures and the incision site closed using 9-mm wound clips.

Certain rats received a daily subcutaneous injection of immunosuppressive cocktail, consisting of 1.0 mg/kg FK506 and 0.5 mg/kg SEW2871 (Cayman Chemical, Ann Arbor, MI),[10] starting the day before implantation and continuing for 8 weeks. In the first series of experiments, 28 wild-type rats received grafts from syngeneic GFP^+ donors but did not receive immunosuppression. In a second series, GFP^+ muscle grafts were implanted into 4 GFP^+ recipients, and 7 wild-type rats received GFP^+ grafts along with the immunosuppressive cocktail.

Radiographic Evaluation

Serial, weekly radiography using a digital dental X-ray unit was performed under general anesthesia to evaluate bone regeneration in the defects. Rats were ventrally positioned and the X-ray sensor was placed under the defect area of each femur. Complete, partial, or no bridging of the defects was determined by inspection of the resulting radiographs by two independent, blinded observers.

μCT

The architecture of newly formed bone in the rat defects was examined with a desktop micro-tomographic imaging system (μCT40, Scanco Medical AG, Bassersdorf, Switzerland) equipped with a 10-mm focal spot microfocus X-ray tube. Femoral defects were scanned using a 20-mm isotropic voxel size, at 55 keV energy, 200-ms integration time, with approximately 500 μCT slices per specimen. The slices were converted to DICOM format using the μCT40 software and then imported for analysis using AnalyzePro (AnalyzeDirect, Overland Park, KS) software. Bone structure was segmented by automated thresholding, separating the bone from the surrounding tissue, and common bone morphometric indices were calculated using the Bone Microarchitecture Analysis module in the AnalyzePro software. Evaluation of only a 4-mm (200 slices)

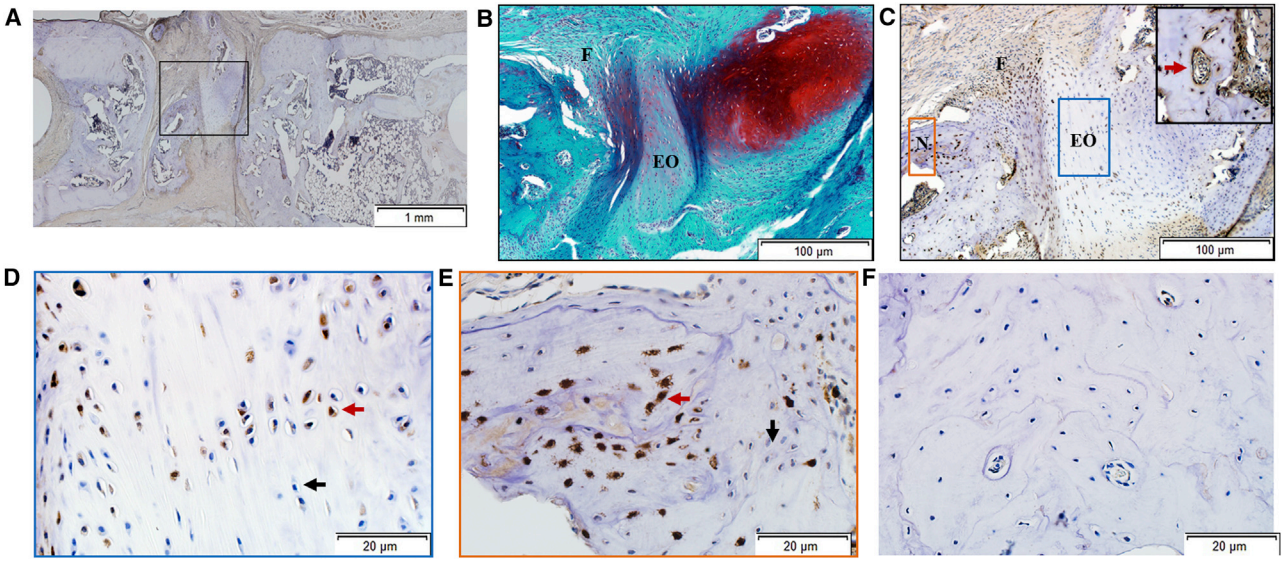

Figure 7. Immunohistochemical Analysis of Defects Where Partial Bridging Occurred

(A–F) As confirmed in (A), although some new bone was formed in the defect, bridging was incomplete. In addition to new bone, the defect contained cartilage, fibrous tissue, and areas that appeared to be undergoing endochondral ossification (B, stained with SOFG). Chondrocytes within the cartilage were GFP^-, whereas cells in areas undergoing endochondral ossification and cells within fibrous tissue contained both GFP^+ and GFP^- cells (C–E). Both GFP^+ cells (example indicated by red arrowhead) and GFP^- cells (example indicated by black arrowhead) were present in the newly formed bone (D and E). Certain blood vessels were lined with GFP^+ cells (insert, C, red arrowhead). (A) and (C)–(E) were stained with anti-GFP antibody. Isotype controls were negative for GFP staining (F). N, new bone; F, fibrous tissue; EO, endochondral ossification.

central region of the defects was used to exclude any pre-existing intact cortical bone. Total volume of the callus size of the defect (TV, mm^3), bone volume (BV, mm^3), BV/TV fraction, and polar moment of inertia (mm4) were calculated from μCT images. Images were thresholded using an adaptive-iterative algorithm, and morphometric variables were computed from the binarized images using direct, 3D techniques that do not rely on any prior assumptions about the underlying structure.

DXA

DXA measurements (bone mineral content [BMC], g) of the defect area were obtained with PIXImus2 apparatus (GE-Lunar, Madison, WI, USA). Briefly, each femoral defect was placed on a lucite block during scanning to simulate soft tissue. The scans were acquired using small animal high-resolution mode. All specimens were evaluated at 8 weeks in the area corresponding to the region of the critical-sized bone defect.

Histology

Femora were fixed in 10% neutral-buffered formalin solution for 72 hr. All samples were decalcified with EDTA 10% solution (pH. 7.4), with constant gentle agitation at room temperature for 30 days. The EDTA solution was replaced by freshly prepared solution every 5 days. The endpoint of decalcification was tested by radiographic methods as decalcification proceeded. Fixed and decalcified specimens were dehydrated in a series of graded ethanol and then embedded in paraffin; 5-μm sections were cut using an automatic microtome (HM 355S, Thermo Scientific, Kalamazoo, MI) and mounted onto positively charged slides (Superfrost Plus Microscope Slides, Fisher Scientific, Pittsburgh, PA).

H&E and safranin O/fast green (SOFG) staining were performed according to standard protocols on paraffin-embedded sections. Briefly, 5-μm paraffin-embedded sections were deparaffinized and rehydrated through a series of xylenes and graded alcohols, followed by staining with hematoxylin for 3 min (Richard-Allan Scientific, Kalamazoo, MI). Slides were then submersed for 45 s in eosin Y (Richard-Allan Scientific, Kalamazoo, MI), then quickly dehydrated in graded ethyl alcohol series, cleared with xylene, and mounted with xylene-based mounting medium (Richard-Allan Scientific, Kalamazoo, MI).

SOFG staining was performed by staining in Weigert's iron hematoxylin for 10 min (Electron Microscopy Sciences, Hatfield, PA), followed by 0.4% aqueous fast green (Sigma-Aldrich, St. Louis, MO) for 4 min and 0.125% safranin O (Electron Microscopy Sciences, Hatfield, PA) for 5 min, then quickly dehydrated in graded ethyl alcohol series, cleared with xylene, and mounted with xylene-based mounting medium. Bright-field images were acquired using an automated inverted microscope (Olympus IX83 microscope, Waltham, MA). Images were stitched at 4× magnification using the cellSense Olympus imaging software, and the data were exported as virtual slide image (vsi) file format.

Immunohistochemistry

Formalin-fixed tissue sections (5 μm) were deparaffinized and rehydrated as described above, then washed twice for 5 min in PBS.

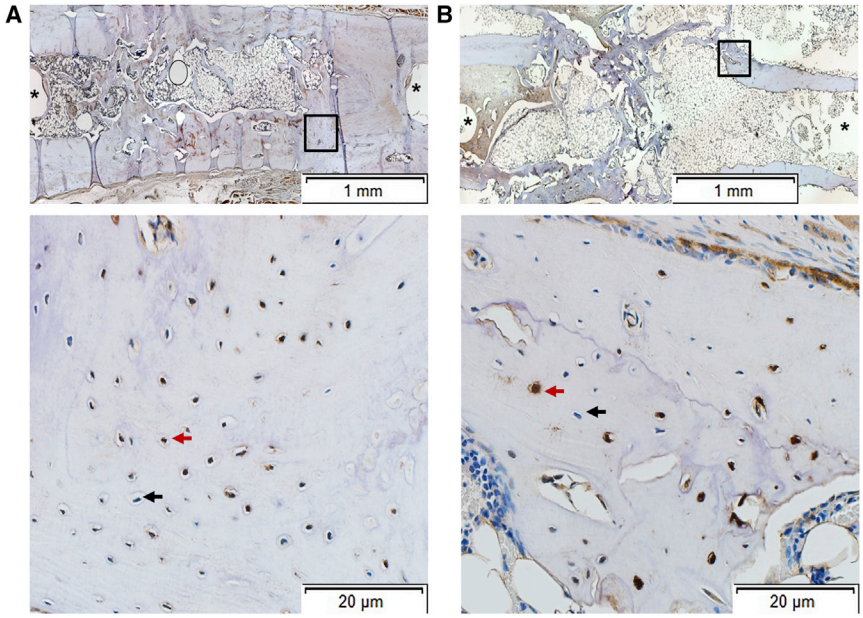

Figure 8. Immunohistochemical Analysis of Defects that Bridged

(A and B) Areas from two different bridged defects (A and B) are shown. Boxed areas in the upper panels are shown at higher magnification in the lower panels, which show that both GFP^+ (example indicated by red arrowhead) and GFP^- (example indicated by black arrowhead) cells are present. Isoptype control staining was negative (data not shown). Asterisks show sites of pinholes.

Nonspecific binding was blocked in 5% rabbit serum. Slides were incubated with rabbit polyclonal anti-GFP antibody (dilution 1:1,000, Ab290, Abcam, Cambridge, MA) overnight at 4°C. The next day, slides were washed four times in PBS for 10 min and incubated with biotinylated goat anti-rabbit IgG antibody (1:300 dilution, BA-1000, Vector Laboratories, Burlingame, CA) for 2 hr at room temperature, followed by detection with an avidin-biotin-based peroxidase kit (Vectastain Elite ABC HRP Kit, Vector Laboratories, Burlingame, CA). Nonspecific background was greatly reduced by pre-treatment of slides with hydrogen peroxidase before incubation with secondary antibody. The antigen-antibody complex was observed by reaction with 3, 3′-diaminobenzidine peroxidase substrate (ImmPACT DAB, Vector Laboratories, Burlingame, CA) and counterstained with hematoxylin (Vector Laboratories, Burlingame, CA). Controls consisting of rabbit IgG polyclonal isotype (dilution 1:1,000, ab27478, Abcam, Cambridge, MA) were included for each section. Positive controls consisted of formalin-fixed, paraffin-embedded femora from transgenic rats expressing GFP.

Two samples from the partial bridging group and two from the complete bridging group were randomly selected for counting the numbers of host and donor cells by two blinded observers. A six-square grid dividing the newly formed bone into areas proximal, middle, and distal to the femoral head was added to two different histological images separated by 10 μm per group. All cells inside lacunae that stained with anti-GFP antibody were designated as donor cells, while cells stained with hematoxylin were designated as host cells. Numbers from both samples were averaged and SDs calculated.

Transcript Expression

Semiquantitative RT-PCR was used to measure the expression of genes associated with osteogenesis, including ALP, Runx2, type I collagen (Col1A1), osteopontin, and osteocalcin, and to monitor the expression of human and rat BMP-2 transcripts. At 28 days after Ad.BMP-2 transduction, cultures of muscle discs were separately flash-frozen in liquid nitrogen and pulverized in pre-chilled grinding jars using a TissueLyser II homogenizer (QIAGEN, Germantown, MD). The RNA fraction was isolated using TRIzol Reagent (Thermo Fisher Scientific, Waltham, MA). RNA concentrations were quantified from the absorbance at 260 nm. RNA (0.5–1 μg) was reverse-transcribed into cDNA using the High Capacity cDNA Reverse Transcription Kit (Thermo Fisher Scientific) and random primers. RT-PCR was performed with an Mx3000PTM thermal cycler (Stratagene, Cedar Creek, TX) using the PowerUp SYBR Green Master Mix kit (Thermo Fisher Scientific). For SYBR Green PCR reactions, the mixture contained 1× SYBR Green, 10 ng cDNA, and 0.5-μM concentrations of each primer. The forward and reverse primers used are listed in Table S2. After uracil-DNA-glycosylase (UDG) activation for 2 min at 50°C and Dual-Lock DNA polymerase activation for 2 min at 95°C, cDNA was amplified in 40 cycles of two steps: 95°C for 15 s and 60°C for 60 s. Melting-curve analyses were performed at the end of each amplification step. The mRNA expression levels were normalized to those of the internal standard GAPDH, and they were reported as relative values (ΔΔCT) to those of non-transduced muscle discs. A relative quantification method using PCR efficiency correction was used as previously described.[36] Primer PCR efficiency is documented in Table S2.

Statistical Analysis

In vitro experiments were repeated at least 4 times using muscle from different donor rats. Representative results are shown as box and whisker plots. For in vitro quantitative results, pairwise comparisons were performed using the Mann-Whitney U test. Data obtained during μCT evaluation was analyzed using a one-way ANOVA with a Bonferroni post hoc analysis; p values less than 0.05 were considered statistically significant.

SUPPLEMENTAL INFORMATION

Supplemental Information includes one figure and two tables and can be found with this article online at https://doi.org/10.1016/j.ymthe.2017.10.001.

AUTHOR CONTRIBUTIONS

R.E.D.L.V. performed surgeries, muscle transduction, X-rays, μCT, data analysis, and manuscript editing. C.L.D.P. performed histology, immunohistochemistry, and manuscript editing. M.T. performed immunohistochemistry, μCT, and manuscript editing. N.Q. performed μCT and manuscript editing. R.M.P. performed surgeries, project development, project oversight, vector production, muscle transduction, RT-PCR, data analysis, and manuscript editing. C.H.E. conceived and developed the project and performed project oversight, data analysis, and manuscript writing and editing. E.F. performed surgeries, project development, project oversight, vector production, muscle transduction, RT-PCR, and manuscript editing.

CONFLICTS OF INTEREST

The authors have no conflicts of interest.

ACKNOWLEDGMENTS

This work was supported by NIH/NIAMS grant R01 AR050243 and the AO Foundation.

REFERENCES

1. Verrier, S., Alini, M., Alsberg, E., Buchman, S.R., Kelly, D., Laschke, M.W., Menger, M.D., Murphy, W.L., Stegemann, J.P., Schütz, M., et al. (2016). Tissue engineering and regenerative approaches to improving the healing of large bone defects. Eur. Cell. Mater. *32*, 87–110.
2. Evans, C.H. (2013). Advances in regenerative orthopedics. Mayo Clin. Proc. *88*, 1323–1339.
3. Walmsley, G.G., Ransom, R.C., Zielins, E.R., Leavitt, T., Flacco, J.S., Hu, M.S., Lee, A.S., Longaker, M.T., and Wan, D.C. (2016). Stem Cells in Bone Regeneration. Stem Cell Rev. *12*, 524–529.
4. Lieberman, J.R., Ghivizzani, S.C., and Evans, C.H. (2002). Gene transfer approaches to the healing of bone and cartilage. Mol. Ther. *6*, 141–147.
5. Evans, C.H., and Huard, J. (2015). Gene therapy approaches to regenerating the musculoskeletal system. Nat. Rev. Rheumatol. *11*, 234–242.
6. Glatt, V., Miller, M., Ivkovic, A., Liu, F., Parry, N., Griffin, D., Vrahas, M., and Evans, C. (2012). Improved healing of large segmental defects in the rat femur by reverse dynamization in the presence of bone morphogenetic protein-2. J. Bone Joint Surg. Am. *94*, 2063–2073.
7. Kaplan, F.S., Pignolo, R.J., and Shore, E.M. (2016). Granting immunity to FOP and catching heterotopic ossification in the Act. Semin. Cell Dev. Biol. *49*, 30–36.
8. Ranganathan, K., Loder, S., Agarwal, S., Wong, V.W., Forsberg, J., Davis, T.A., Wang, S., James, A.W., and Levi, B. (2015). Heterotopic Ossification: Basic-Science Principles and Clinical Correlates. J. Bone Joint Surg. Am. *97*, 1101–1111.
9. Shore, E.M., Xu, M., Feldman, G.J., Fenstermacher, D.A., Cho, T.J., Choi, I.H., Connor, J.M., Delai, P., Glaser, D.L., LeMerrer, M., et al. (2006). A recurrent mutation in the BMP type I receptor ACVR1 causes inherited and sporadic fibrodysplasia ossificans progressiva. Nat. Genet. *38*, 525–527.
10. Liu, F., Ferreira, E., Porter, R.M., Glatt, V., Schinhan, M., Shen, Z., Randolph, M.A., Kirker-Head, C.A., Wehling, C., Vrahas, M.S., et al. (2015). Rapid and reliable healing of critical size bone defects with genetically modified sheep muscle. Eur. Cell. Mater. *30*, 118–130.
11. Evans, C.H., Liu, F.J., Glatt, V., Hoyland, J.A., Kirker-Head, C., Walsh, A., Betz, O., Wells, J.W., Betz, V., Porter, R.M., et al. (2009). Use of genetically modified muscle and fat grafts to repair defects in bone and cartilage. Eur. Cell. Mater. *18*, 96–111.
12. Lois, C., Hong, E.J., Pease, S., Brown, E.J., and Baltimore, D. (2002). Germline transmission and tissue-specific expression of transgenes delivered by lentiviral vectors. Science *295*, 868–872.
13. Evans, C.H. (2015). Native, living tissues as cell seeded scaffolds. Ann. Biomed. Eng. *43*, 787–795.
14. Bosch, P., Musgrave, D.S., Lee, J.Y., Cummins, J., Shuler, F., Ghivizzani, S.C., Evans, E., Robbins, P.D., and Huard, J. (2000). Osteoprogenitor cells within skeletal muscle. J. Orthop. Res. *18*, 933–944.
15. Brack, A.S., and Rando, T.A. (2012). Tissue-specific stem cells: lessons from the skeletal muscle satellite cell. Cell Stem Cell *10*, 504–514.
16. Lemos, D.R., Eisner, C., Hopkins, C.I., and Rossi, F.M.V. (2015). Skeletal muscle-resident MSCs and bone formation. Bone *80*, 19–23.
17. Gates, C.B., Karthikeyan, T., Fu, F., and Huard, J. (2008). Regenerative medicine for the musculoskeletal system based on muscle-derived stem cells. J. Am. Acad. Orthop. Surg. *16*, 68–76.
18. Lounev, V.Y., Ramachandran, R., Wosczyna, M.N., Yamamoto, M., Maidment, A.D., Shore, E.M., Glaser, D.L., Goldhamer, D.J., and Kaplan, F.S. (2009). Identification of progenitor cells that contribute to heterotopic skeletogenesis. J. Bone Joint Surg. Am. *91*, 652–663.
19. Berendsen, A.D., and Olsen, B.R. (2015). Bone development. Bone *80*, 14–18.
20. Ferguson, C.M., Miclau, T., Hu, D., Alpern, E., and Helms, J.A. (1998). Common molecular pathways in skeletal morphogenesis and repair. Ann. N Y Acad. Sci. *857*, 33–42.
21. Gibson, G. (1998). Active role of chondrocyte apoptosis in endochondral ossification. Microsc. Res. Tech. *43*, 191–204.
22. Yang, L., Tsang, K.Y., Tang, H.C., Chan, D., and Cheah, K.S. (2014). Hypertrophic chondrocytes can become osteoblasts and osteocytes in endochondral bone formation. Proc. Natl. Acad. Sci. USA *111*, 12097–12102.
23. Hu, D.P., Ferro, F., Yang, F., Taylor, A.J., Chang, W., Miclau, T., Marcucio, R.S., and Bahney, C.S. (2017). Cartilage to bone transformation during fracture healing is coordinated by the invading vasculature and induction of the core pluripotency genes. Development *144*, 221–234.
24. Bahney, C.S., Hu, D.P., Taylor, A.J., Ferro, F., Britz, H.M., Hallgrimsson, B., Johnstone, B., Miclau, T., and Marcucio, R.S. (2014). Stem cell-derived endochondral cartilage stimulates bone healing by tissue transformation. J. Bone Miner. Res. *29*, 1269–1282.
25. Musgrave, D.S., Bosch, P., Ghivizzani, S., Robbins, P.D., Evans, C.H., and Huard, J. (1999). Adenovirus-mediated direct gene therapy with bone morphogenetic protein-2 produces bone. Bone *24*, 541–547.
26. Betz, O.B., Betz, V.M., Nazarian, A., Pilapil, C.G., Vrahas, M.S., Bouxsein, M.L., Gerstenfeld, L.C., Einhorn, T.A., and Evans, C.H. (2006). Direct percutaneous gene delivery to enhance healing of segmental bone defects. J. Bone Joint Surg. Am. *88*, 355–365.
27. Egermann, M., Baltzer, A.W., Adamaszek, S., Evans, C., Robbins, P., Schneider, E., and Lill, C.A. (2006). Direct adenoviral transfer of bone morphogenetic protein-2 cDNA enhances fracture healing in osteoporotic sheep. Hum. Gene Ther. *17*, 507–517.
28. Egermann, M., Lill, C.A., Griesbeck, K., Evans, C.H., Robbins, P.D., Schneider, E., and Baltzer, A.W. (2006). Effect of BMP-2 gene transfer on bone healing in sheep. Gene Ther. *13*, 1290–1299.
29. Yang, Y., Nunes, F.A., Berencsi, K., Furth, E.E., Gönczöl, E., and Wilson, J.M. (1994). Cellular immunity to viral antigens limits E1-deleted adenoviruses for gene therapy. Proc. Natl. Acad. Sci. USA *91*, 4407–4411.
30. Reinke, S., Geissler, S., Taylor, W.R., Schmidt-Bleek, K., Juelke, K., Schwachmeyer, V., Dahne, M., Hartwig, T., Akyüz, L., Meisel, C., et al. (2013). Terminally differentiated $CD8^+$ T cells negatively affect bone regeneration in humans. Sci. Transl. Med. *5*, 177ra36.
31. Spiekerkoetter, E., Tian, X., Cai, J., Hopper, R.K., Sudheendra, D., Li, C.G., El-Bizri, N., Sawada, H., Haghighat, R., Chan, R., et al. (2013). FK506 activates BMPR2, rescues endothelial dysfunction, and reverses pulmonary hypertension. J. Clin. Invest. *123*, 3600–3613.
32. Kugimiya, F., Yano, F., Ohba, S., Igawa, K., Nakamura, K., Kawaguchi, H., and Chung, U.I. (2005). Mechanism of osteogenic induction by FK506 via BMP/Smad pathways. Biochem. Biophys. Res. Commun. *338*, 872–879.

33. Evans, C.H., Palmer, G.D., Pascher, A., Porter, R., Kwong, F.N., Gouze, E., Gouze, J.N., Liu, F., Steinert, A., Betz, O., et al. (2007). Facilitated endogenous repair: making tissue engineering simple, practical, and economical. Tissue Eng. *13*, 1987–1993.

34. Gouze, J.N., Stoddart, M.J., Gouze, E., Palmer, G.D., Ghivizzani, S.C., Grodzinsky, A.J., and Evans, C.H. (2004). In vitro gene transfer to chondrocytes and synovial fibroblasts by adenoviral vectors. Methods Mol. Med. *100*, 147–164.

35. Brown, K.V., Li, B., Guda, T., Perrien, D.S., Guelcher, S.A., and Wenke, J.C. (2011). Improving bone formation in a rat femur segmental defect by controlling bone morphogenetic protein-2 release. Tissue Eng. Part A *17*, 1735–1746.

36. Pfaffl, M.W. (2001). A new mathematical model for relative quantification in real-time RT-PCR. Nucleic Acids Res. *29*, e45.

YMTHE, Volume *26*

Supplemental Information

Contribution of Implanted, Genetically Modified Muscle Progenitor Cells Expressing BMP-2 to New Bone Formation in a Rat Osseous Defect

Rodolfo E. De La Vega, Consuelo Lopez De Padilla, Miguel Trujillo, Nicholas Quirk, Ryan M. Porter, Christopher H. Evans, and Elisabeth Ferreira

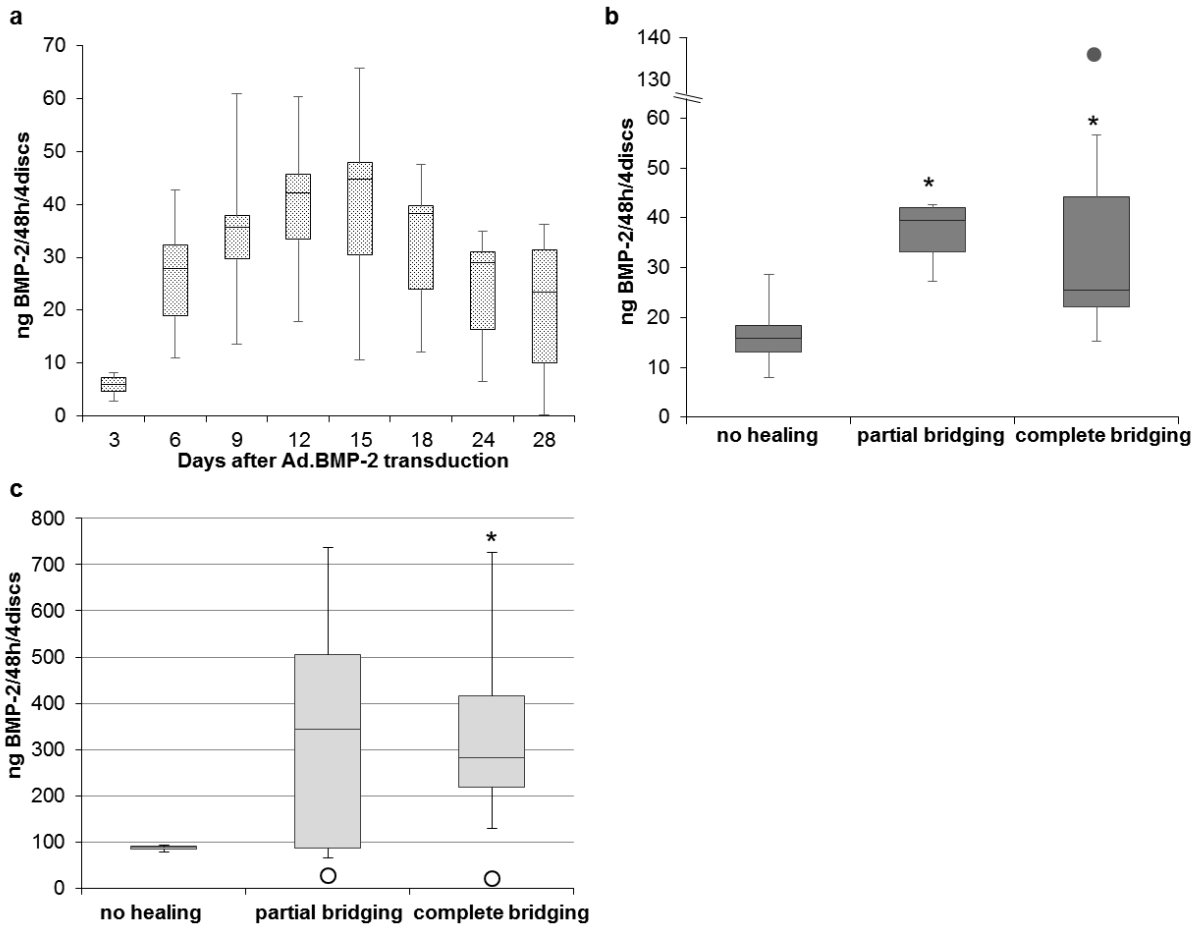

Figure S1: BMP-2 production by genetically modified rat muscle discs. BMP-2 was quantified in muscle supernatants using an ELISA kit specific for the human protein. (a) Time course of BMP-2 production *in vitro* by cultures of transduced muscle discs (n=8). (b) BMP-2 secretion by muscle discs at day 3 after Ad.BMP-2 transduction (n>8 per group) correlated to radiographic evaluation of repair 8 weeks after implantation. (c) BMP-2 secretion by muscle discs at the time of implantation (i.e., day 5 after transduction), correlated to radiographic evaluation of repair 8 weeks after implantation. Representative results are shown as box and whisker plots, with median as the horizontal bar, interquartile range calculated using Tukey hinges as the box, and the lowest and highest values represented as whiskers Circle dots represent outliers. * denotes a significant difference ($p < 0.05$) compared to the "no healing" group.

Rat Number	Recipient	FK506 /SEW 2871	BMP-2 secretion (ng/48h/4discs)	Radiologic Bridging
1	Wild-type	+	220.5 ± 14.0	Complete
2	Wild-type	+	726.2 ± 35.1	Complete
3	Wild-type	+	219.8 ± 11.4	Complete
4	Wild-type	+	344.3 ± 16.4	Complete
5	Wild-type	+	129.3 ± 2.1	Complete
6	Wild-type	+	415.8 ± 2.4	Complete
7	Wild-type	+	415.1 ± 16.02	Complete
8	GFP	-	283.2 ± 33.5	Partial
9	GFP	-	405.4 ± 51.5	Partial
10	GFP	-	284.6 ± 21.4	None (pin loosening)
11	GFP	-	737.7 ± 20.1	Partial

Table S1. Bridging of femoral defects in wild-type and GFP^+ rats by the implantation of muscle discs from GFP^+ rats expressing BMP-2 in the absence or presence of immunosuppression

Gene	Accession number	Primer sequence 5'-3'	Product size (bp)	Primer efficiency
Rat GAPDH	NM 017008	F : GGTCGGTGTGAACGGATTTGG R : GCCGTGGGTAGAGTCATACTGGAC	148	95%
Rat ALP	NM 013059	F : ATGTCTGGAACCGCACTGAAC R : TTCTTTGTCAGGATCCGGAGG	166	99%
Rat Runx2	NM 001278483	F : GCCAGGTTCAACGATCTGAG R : GAGGCGGTCAGAGAACAAAC	201	95%
Rat Col1A1	NM 053304	F : CTGACTGGAAGAGCGGAGAG R : GAGTGGGGAACACACAGGTC	111	96%
Rat osteopontin	M99252	F : AAGCCTGACCCATCTCAGAA R : ATGGCTTTCATTGGAGTTGC	114	98%
Rat osteocalcin	NM 013414	F : GCATTCTGCCTCTCTGACCT R : GGCTCCAAGTCCATTGTTGA	132	95%
Rat BMP-2	NM 017178	F : TAAAGCCTGCCACAGCCAGC R : TGTCCATCGCATCACAGCCG	122	98%
Human BMP-2	NM 001200	F : AACACTGTGCGCAGCTTCC R : CTCCGGGTTGTTTTCCCAC	74	96%

Table S2. List and sequences of primers used for analysis of mRNA expression. Forward (F). Reverse (R).